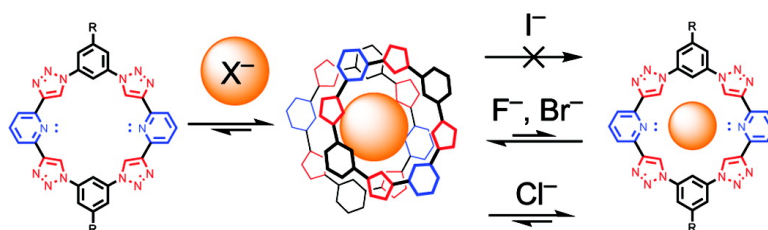


## Dipole-Promoted and Size-Dependent Cooperativity between Pyridyl-Containing Triazolophanes and Halides Leads to Persistent Sandwich Complexes with Iodide

Yongjun Li, Maren Pink, Jonathan A. Karty, and Amar H. Flood

*J. Am. Chem. Soc.*, **2008**, 130 (51), 17293-17295 • DOI: 10.1021/ja8077329 • Publication Date (Web): 03 December 2008

Downloaded from <http://pubs.acs.org> on February 8, 2009



### More About This Article

Additional resources and features associated with this article are available within the HTML version:

- Supporting Information
- Access to high resolution figures
- Links to articles and content related to this article
- Copyright permission to reproduce figures and/or text from this article

[View the Full Text HTML](#)

## Dipole-Promoted and Size-Dependent Cooperativity between Pyridyl-Containing Triazolophanes and Halides Leads to Persistent Sandwich Complexes with Iodide

Yongjun Li,<sup>†</sup> Maren Pink, Jonathan A. Karty, and Amar H. Flood\*

Department of Chemistry, Indiana University, Bloomington, 800 East Kirkwood Avenue, Bloomington, Indiana 47405

Received September 30, 2008; E-mail: aflood@indiana.edu

Encapsulation of a guest by the cooperative dimerization of a host to form “sandwich” complexes is an effective means to increase dimensionality<sup>1</sup> for optimizing complex stability. Lessons provided by crown ether binding with alkali metals<sup>2</sup> indicate the importance of a size difference between an ion and the cavity of the receptor for forming sandwiches. This mismatch provides a means to decrease the stability of the 1:1 complex ( $K_1$ ) relative to the 2:1 ( $K_2$ ). The relative magnitudes of  $K_1$  and  $K_2$  thereby provide insights into cooperative effects.<sup>3</sup> Only a few 2:1 sandwich complexes are known for anionic guests. Here, the 1:1 and 2:1 complexes are observed either depending upon the stoichiometry in solution<sup>4</sup> or solely as 2:1 complexes in the solid state.<sup>5</sup> Only an “anti-crown” mercuracarborand<sup>6</sup> shows only 2:1 sandwiches in solution with halides; however, the binding constants were not characterized. Cooperativity has been quantified<sup>4</sup> in two instances to result from interactions between receptors. Here we present findings on a new class of triazolophane<sup>7</sup> incorporating pyridyl ring systems (Figure 1) that forms strong and persistent 2:1 complexes with the large  $I^-$  ion in solution. Quantitative binding studies with  $F^-$ ,  $Cl^-$ , and  $Br^-$  show both 2:1 and 1:1 complexes implicating the importance of the electronic character of the cavity in modulating cooperativity.

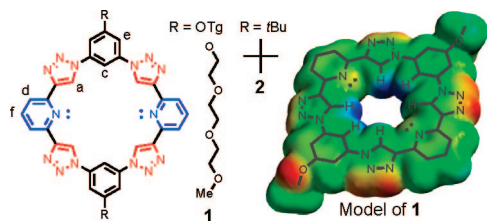


**Figure 1.** Representations of pyridyl-containing triazolophanes **1** and **2**, and the electrostatic potential surface of a model of **1** (blue sections represent regions of positive electrostatic character).

Prior studies on tetraphenylene-based triazolophanes<sup>7,8</sup> show size-dependent 1:1 binding with halides ( $Cl^- > Br^- > F^- \gg I^-$ ), using only  $CH \cdots X^-$  hydrogen bonding,<sup>9</sup> and a propensity for self-association. Molecular modeling indicated the  $I^-$  ion was not fully encapsulated. This tendency could lead<sup>2</sup> to dimerization-induced binding of iodide ions, yet the 2:1 complexes were not observed. To elaborate on this idea, pyridyl ring systems were considered as a replacement for the phenylenes. Pyridines have been used previously<sup>8b,10</sup> to alter the electronic character and size of binding sites. Consequently, compounds **1** and **2** were designed with pyridyl rings replacing the C-linked phenylenes in the west and east directions. Modeling (HF/3-21G) confirms the predictions: Pyridyls generate negative electrostatic potentials inside the cavity (Figure 1) and the cavity becomes oval (the vertical axis gets smaller by  $\sim 0.3 \text{ \AA}$  and the horizontal axis increases by  $> 0.2 \text{ \AA}$ ). We

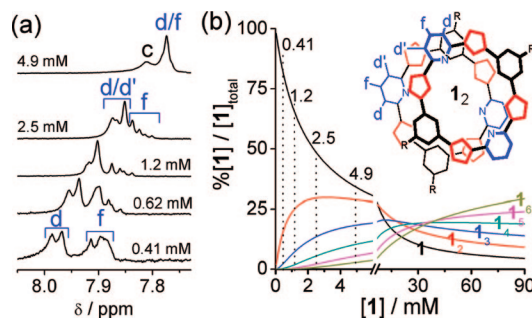


**Figure 2.** (a)  $^1H$  NMR spectra of **1** (pyridyl region) as a function of concentration ( $CD_2Cl_2$ , 298 K, 400 MHz) and (b) calculated speciation curves for self-association up to the hexamer **1<sub>6</sub>** with  $K_E = 255 \text{ M}^{-1}$

hypothesize that the cumulative effect of these features will destabilize the 1:1 complex in favor of the 2:1 sandwich.

The triazolophanes were prepared following prior methods<sup>7</sup> of symmetric chain extension followed by macrocyclization under conditions of high dilution and Cu(I) catalysis. The electrospray ionization mass spectrometry (ESI-MS) and  $^1H$  NMR spectra confirm<sup>11</sup> the identity of the triazolophane.

Triazolophane **2** was only soluble as the tetrabutylammonium (TBA) salt:  $[2_2 \cdot I^-]TBA$ . Crystals grown for X-ray analysis diffract weakly. A partial solution<sup>11</sup> shows (a) formation of the 2:1 sandwich with the  $I^-$  ion located between both triazolophanes, (b) the triazolophanes within  $\pi$  stacking distance ( $3.4 \text{ \AA}$ ), and (c) that the angle of rotation ( $\theta$ ) between the two triazolophanes is  $\sim 56^\circ$ .

The triazolophane **1** was examined in dichloromethane for its propensity to self-associate using both  $^1H$  NMR (Figure 2) and UV studies.<sup>11</sup> The aromatic protons shift upfield with concentration (0.4–90 mM) indicating  $\pi$ -stacking and leading to the self-association constant,<sup>11</sup>  $K_E = 255 \pm 70 \text{ M}^{-1}$ . Consistently,<sup>7b</sup> continual changes in the diffusion coefficient<sup>11</sup> are observed from 2 to 100 mM. Modeling<sup>12</sup> of the equilibria shows that with increasing concentration (Figure 2b), the amount of monomer decreases and the dimer shows a maximum in its population at  $\sim 3$  mM, thereafter, both species are replaced by higher order species. The splitting pattern in the pyridyl region of the  $^1H$  NMR spectra (Figure 2a) agrees with this picture. At 0.41 mM, the pyridyl  $H^d$  and  $H^f$  protons are observed to form an  $A_2X$  spin system corresponding to the monomer **1**. This pattern transforms into an ABC spin system at 2.5 mM, which can arise when the two  $H^d$  protons are no longer equivalent as expected (inset, Figure 2b) from a rotated ( $0^\circ < \theta < 90^\circ$ ),  $\pi$ -stacked pair of triazolophanes, **1<sub>2</sub>**. A doublet of doublets ( $H^f$ ) sits upfield from the partially overlapping doublets of the inequivalent  $H^d$  and  $H^{d'}$  protons. At 4.9 mM, a broad singlet replaces the ABC pattern indicating a shift to rapidly equilibrating higher-order aggregates. The UV spectra of **1** ( $2 \mu\text{M}$ –1 mM) show a decrease in the normalized intensities consistent with self-association.<sup>7b</sup> We attribute the rotated configuration in **1<sub>2</sub>** to

<sup>†</sup> Present address: CAS Key Laboratory of Organic Solids, Institute of Chemistry, CAS, Beijing, 10080, P. R. China.

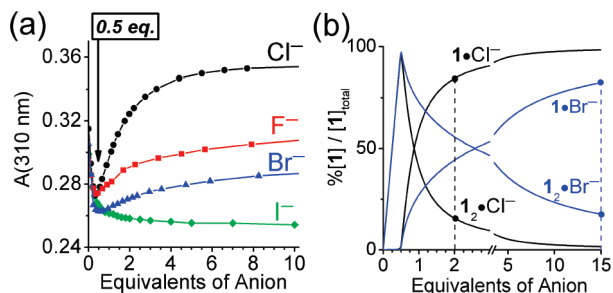


**Figure 3.** (a) UV binding curves for **1** (20 μM) with halides (CH<sub>2</sub>Cl<sub>2</sub>, 298 K) and (b) the speciation curves calculated<sup>12</sup> from  $K_1$  and  $K_2$  (Table 1) for Cl<sup>-</sup> and Br<sup>-</sup> at 5 mM.

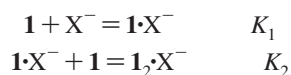
electrostatic complementarity between the opposite dipoles on the pyridines (-2.4 D) and the triazoles (+5.0 D) of the triazolophane dimer pair.

Halide binding was investigated using UV titration (Figure 3a). Upon addition of F<sup>-</sup>, Cl<sup>-</sup>, and Br<sup>-</sup> to **1** (20 μM) the absorbance decreases to a minimum at 0.5 equiv as a consequence of the  $\pi$ -stacked structure in the 2:1 complex. The absorbance then increases with the addition of more halide leading to the 1:1 complex. For I<sup>-</sup>, the peak intensity decreases continuously during the titration. When repeated at 1 μM,<sup>11</sup> addition of F<sup>-</sup>, Cl<sup>-</sup>, and Br<sup>-</sup> appears to proceed directly to the 1:1 complex while only I<sup>-</sup> forms the 2:1 sandwich.

**Table 1.** Binding Energies (kcal mol<sup>-1</sup>, ±10%) between **1** (20 μM) and the TBA Halides in CH<sub>2</sub>Cl<sub>2</sub> Determined by Equilibrium-Restricted Factor Analysis of UV Titration Data

	$\Delta G_1$ ( $K_1/M^{-1}$ )	$\Delta G_2$ ( $K_2/M^{-1}$ )	$\Delta G$ ( $\beta_2/M^{-2}$ )
F <sup>-</sup>	-7.4 (275 000)	-7.6(380 000)	
Cl <sup>-</sup>	-8.5(1 600 000)	-7.2(190 000)	
Br <sup>-</sup>	-7.5 (315 000)	-7.9(580 000)	
I <sup>-</sup>			-14.9(8.6 × 10 <sup>10</sup> )

Quantitative analysis of the UV titration data was conducted using an equilibrium-restricted factor analysis<sup>13</sup> of the entire wavelength range<sup>11</sup> to characterize the binding constants (Table 1). The models used the stepwise formation equilibria



or the direct formation of the sandwich complex



For the I<sup>-</sup> ion, the best fit was obtained from the direct formation of the 2:1 dimer ( $\beta_2$ ) at both concentrations. At the higher concentration, the titration data for F<sup>-</sup>, Cl<sup>-</sup>, and Br<sup>-</sup> are best fit with the stepwise equilibria ( $K_1$  and  $K_2$ ): The data obtained from the 20 μM titration contains reasonable proportions of all three absorbers, **1**, **1**<sub>2</sub>·X<sup>-</sup> and **1**·X<sup>-</sup>, and is under moderate binding conditions,<sup>14</sup> therefore, it is more accurate than fitting the data at either lower (1 μM) or higher (5 mM, NMR) concentrations. The accuracy of these models was confirmed by inspecting the speciation curves calculated<sup>11</sup> from the  $K_1$ ,  $K_2$ , and  $\beta_2$  values. At 1 μM, these curves confirm that the 2:1 complex is present at <10%, consistent with its apparent absence in the fitting.

The relative values of  $K_1$  and  $K_2$ , as well as the behavior of I<sup>-</sup>, indicate<sup>3</sup> that positive cooperativity follows the order I<sup>-</sup> ≪ Br<sup>-</sup> < F<sup>-</sup> whereas Cl<sup>-</sup> displays negative cooperativity. The halides were defined as having two identical binding sites and the triazolophane with one binding site. Statistical binding would occur if  $K_2 = K_1/4$  and deviations higher or lower signify positive and negative

cooperativity, as observed. These cooperative effects were verified graphically utilizing linear Scatchard plots.<sup>11,15</sup>

The 2:1 complex **1**<sub>2</sub>·I<sup>-</sup> is persistent in solution. To estimate the stepwise binding constants, speciation curves<sup>11</sup> were generated<sup>12</sup> for  $K_1$  values while keeping  $\beta_2$  constant. The NMR concentration of 2 mM was used to provide the greatest opportunity of observing the 1:1 complex. This approach generates upper and lower limits:  $K_1 < 3200$  and  $K_2 > 32\,000\,000\text{ M}^{-1}$ . The former concurs with the  $K_1$  value (5000 M<sup>-1</sup>) for the related tetraphenylene triazolophane.<sup>7b</sup>

Solution structures of **1** with halides were characterized (Figure 4) by <sup>1</sup>H NMR spectroscopy (CD<sub>2</sub>Cl<sub>2</sub>, 400 MHz). While different chemical shift behaviors are observed for the various halides, each follows the calculated<sup>11</sup> speciation curves ([**1**] = 5 mM). Upfield and downfield shifts are attributed to the relative importance of  $\pi$ -stacking and halide binding, respectively. In the simplest case, titration of **1** with TBAI (Figure 4a) displays shifts in all positions up to the addition of 0.5 equiv consistent with 2:1 stoichiometry, **1**<sub>2</sub>·I<sup>-</sup>, as confirmed by a Job's Plot.<sup>11</sup> The stability of the sandwich complex is maintained in the presence of 150 equiv of I<sup>-</sup>. The inner triazole (H<sup>a</sup>) and phenylene (H<sup>c</sup>) CH protons both shift downfield by ~0.2 ppm indicating the dominance of I<sup>-</sup> binding on their positions.<sup>7b</sup> The outer protons on the pyridyl rings (H<sup>d</sup> and H<sup>f</sup>) shift modestly downfield while the phenylene H<sup>e</sup> moves slightly upfield, showing the importance of  $\pi$ -stacking. Diffusion NMR is consistent with sandwich formation. Addition of 0.5 equiv of I<sup>-</sup> steps the diffusion coefficient from 3.5 to 3.4 × 10<sup>-10</sup> m<sup>2</sup> cm<sup>-1</sup> where it stays up to 3 equiv.

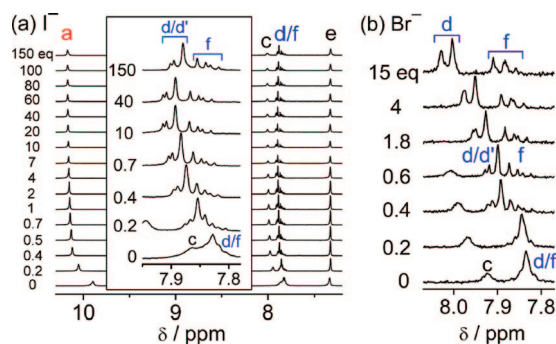


**Figure 4.** <sup>1</sup>H NMR spectra showing the titration of **1** (5 mM, CD<sub>2</sub>Cl<sub>2</sub>, 400 MHz, 298 K) with (a) I<sup>-</sup> (inset, pyridyl region) and (b) Br<sup>-</sup> (pyridyl region).

The solution structure of **1**<sub>2</sub>·I<sup>-</sup> is consistent with dimer **1**<sub>2</sub> and the preliminary crystal structure of [**1**<sub>2</sub>·I]**TBA**. An ABC spin system for the pyridyl protons (inset, Figure 4a) indicates two rotated face-to-face triazolophanes. In support of this geometry, a <sup>1</sup>H-<sup>1</sup>H ROSEY experiment shows through-space cross peaks from (a) the phenylene H<sup>e</sup> and (b) both the  $\alpha$ - and  $\beta$ -methylene protons on the OTg substituent to the pyridyl H<sup>d</sup> and H<sup>d'</sup> protons. In the parent triazolophane, the distances are too large (>6.4 Å) to support an NOE. These observations indicate an average solution structure with a centrally located halide.

The TBACl and TBABr salts behave the same as TBAI up to ~0.5 equiv (e.g., Br<sup>-</sup>, Figure 4b). Further additions indicate the shift from 2:1 to 1:1 complexes with the ABC spin system becoming replaced by the A<sub>2</sub>X system. The relative intensities of these two spin patterns signify the population ratio between the 2:1 and 1:1 species. The point where the A<sub>2</sub>X system dominates occurs at 2.0 equiv for the Cl<sup>-</sup>,<sup>11</sup> whereas for the Br<sup>-</sup> it is as late as 15 equiv, perfectly consistent with the differences in the speciation curves (Figure 3b, dashed lines) between these two halides.

In the case of TBAF, the titration behavior shows<sup>11</sup> a cross over to the  $A_2X$  system beyond 22 equiv. The *shifts* in the proton signals, however, are more complicated than in the  $Cl^-$  and  $Br^-$  cases. Beyond 0.5 equiv all the proton signals except  $H^c$  shift steadily upfield. The upfield shifts normally indicate increasing self-association. Molecular modeling (HF/3-21G)<sup>11</sup> indicates that in the 1:1 complex  $1 \cdot F^-$ , all six CH H-bond donors bind symmetrically with the  $F^-$  ion. Consequently, the proton shifts that occur upon transformation into the 1:1 complex are attributed to the conformational changes of **1** in addition to the effects of halide binding and dedimerization.

Complex formation was confirmed by ESI-MS. The ESI-MS is often taken to reflect the solution species present in solution.<sup>4</sup> The analysis<sup>11</sup> of solutions ( $[1] = 50 \mu M$ ,  $CH_2Cl_2$ ) with 2 equiv of  $Cl^-$  showed the peak for the 1:1 complex stronger than the 2:1. For the  $Br^-$ , the two peaks were equal. Under these conditions, the  $I^-$  sample retained the dominance of its 2:1 dimer peak. These observations agree with the calculated speciation curves<sup>11</sup> and the change from negative ( $Cl^-$ ) to positive cooperativity ( $Br^-$ ,  $I^-$ ). A competition experiment for halide binding with **1** was conducted, in which a solution containing all four halides at 0.125 equiv was analyzed. The peak intensities indicate the relative stabilities of the sandwiches:  $I^- \gg Br^- > Cl^-$ . The  $F^-$  complexes were not observed. In the same spectrum, the 1:1 peaks followed  $Cl^- > Br^- \approx I^-$ . These observations again concur with the speciation curves.

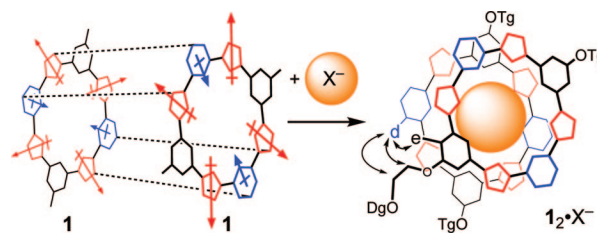
All of the titration data validate the accuracy of the  $K_1$ ,  $K_2$ , and  $\beta_2$  values and the presence of cooperativity. The propensity for 2:1 halide binding by the pyridyl triazolophanes can be best explained by comparison to the tetraphenylene ones.<sup>7b</sup> For the  $Cl^-$  and  $Br^-$  ions, the  $\Delta G_1$  values for **1** are 0.5 and 0.9 kcal mol<sup>-1</sup> lower, respectively, than for the tetraphenylenes.<sup>7b</sup> Modeling (HF/3-21G)<sup>11</sup> shows both 1:1 complexes are planar with the halides fitting snugly inside the cavity. These observations confirm our hypothesis that the lone pairs of electrons on the nitrogens are acting in a destabilizing way. The fact that the 1:1  $Br^-$  complex is more greatly affected is consistent with its larger size and therefore closer proximity to the nitrogen lone pairs.

In the case of  $F^-$ , the 1:1 complex is more stable by 0.3 kcal mol<sup>-1</sup>, which is consistent with the centrally located  $F^-$  ion in **1**: Being able to engage with six CH H-bond donors rather than three, as is the case for tetraphenylenes,<sup>7b</sup> more than overcomes the repulsions from the pyridyl nitrogens. The  $K_2$  value has been measured<sup>13b</sup> for a related tetraphenylene-triazolophane at  $-6$  kcal mol<sup>-1</sup>, which indicates that the 2:1 sandwich dimer has in fact gained in strength by  $\sim 1.5$  kcal mol<sup>-1</sup> for **1**.

Lastly,  $I^-$  binding shows highly positive cooperativity. In contrast to the smaller halides, modeling (HF/3-21G) of the 1:1 complex shows<sup>11</sup> the iodide ion to be less encapsulated in  $1 \cdot I^-$ , relative to the tetraphenylene. This structural feature is a hallmark<sup>2</sup> for favoring sandwich complexes. A calculation on the 1:1 complex shows that the negative electrostatic potentials on the pyridyls are retained in the presence of the  $I^-$  ion. The increase in  $K_2$ , therefore, must stem from the novel configuration of the  $\pi$ -stacked and rotated pair of triazolophanes: Registration between opposite dipoles (pyridine and triazole), which guides the angle of rotation between dimers, also aids in partially extinguishing (Scheme 1) the pyridyl-based repulsions in the 2:1 sandwiches.

The smaller halides fit snugly inside the cavity and they all have similar 2:1 binding strengths (Table I). Consequently, the dipole-stabilized dimers must be primarily responsible for their sandwich formation. Positive cooperativity is seen ( $F^-$ ,  $Br^-$ ) when the 1:1 binding strength is not significant enough to overcome the dimer's affinity. The  $F^-$  is too small and the  $Br^-$  too large for favorable

**Scheme 1.** Representations of the Opposite Dipoles Participating in the Formation of  $1_2 \cdot X^-$ <sup>a</sup>



1:1 complexes. The  $Cl^-$  has large 1:1 binding strength to offset the dimer leading to slight negative cooperativity.

In conclusion, pyridyl units destabilize the 1:1 triazolophane complexes on account of the  $N:\cdots X^-$  electron pair repulsions. In the 2:1 sandwich complexes, the repulsions become reduced by partial cancellation of opposite dipoles. This phenomenon can only occur in the  $\pi$ -stacked dimers. These elements lower  $K_1$  and increase  $K_2$  turning on cooperativity. The size matching between  $F^-$ ,  $Cl^-$ , and  $Br^-$  and the central cavity leads to modest cooperative effects. However, when these factors are coupled to a large size mismatch, highly positive cooperativity leads to the enhanced stability and persistent nature of the  $I^-$  sandwich complex.

**Acknowledgment.** The authors thank D. A. Vander Griend for discussions.

**Supporting Information Available:** Synthesis, characterization, titration, modeling, ESI-MS, and X-ray analyses. This material is available free of charge via the Internet at <http://pubs.acs.org>.

## References

- (1) (a) Hof, F.; Craig, S. L.; Nuckolls, C.; Rebek, J. *Angew. Chem., Int. Ed.* **2002**, *41*, 1488–1508. (b) Kang, S. O.; Hossain, M. A.; Bowman-James, K. *Coord. Chem. Rev.* **2006**, *250*, 3038–3052.
- (2) Bajaj, A. V.; Poonia, N. S. *Coord. Chem. Rev.* **1988**, *87*, 55–213.
- (3) (a) Ercolani, G. *J. Am. Chem. Soc.* **2003**, *125*, 16097–16103. (b) Badjic, J. D.; Nelson, A.; Cantrill, S. J.; Turnbull, W. B.; Stoddart, J. F. *Acc. Chem. Res.* **2005**, *38*, 723–732.
- (4) (a) Choi, K. H.; Hamilton, A. D. *J. Am. Chem. Soc.* **2001**, *123*, 2456–2457. (b) Choi, K. H.; Hamilton, A. D. *J. Am. Chem. Soc.* **2003**, *125*, 10241–10249. (c) Kubik, S.; Goddard, R.; Kirchner, R.; Nolting, D.; Seidel, J. *Angew. Chem., Int. Ed.* **2001**, *40*, 2648–2651. (d) Rodriguez-Docampo, Z.; Pascu, S. I.; Kubik, S.; Otto, S. *J. Am. Chem. Soc.* **2006**, *128*, 11206–11210.
- (5) (a) Hossain, M. A.; Llinares, J. M.; Powell, D.; Bowman-James, K. *Inorg. Chem.* **2001**, *40*, 2936–2937. (b) Custelcean, R.; Remy, P.; Bonnesen, P. V.; Jiang, D. E.; Moyer, B. A. *Angew. Chem., Int. Ed.* **2008**, *47*, 1866–1870.
- (6) (a) Lee, H.; Diaz, M.; Knobler, C. B.; Hawthorne, M. F. *Angew. Chem., Int. Ed.* **2000**, *39*, 776–778. (b) Lee, H.; Knobler, C. B.; Hawthorne, M. F. *J. Am. Chem. Soc.* **2001**, *123*, 8543–8549.
- (7) (a) Li, Y.; Flood, A. H. *Angew. Chem., Int. Ed.* **2008**, *47*, 2649–2652. (b) Li, Y.; Flood, A. H. *J. Am. Chem. Soc.* **2008**, *130*, 12111–12122.
- (8) Also see related foldamers: (a) Jwarkar, H.; Lenhardt, J. M.; Pham, D. M.; Craig, S. L. *Angew. Chem., Int. Ed.* **2008**, *47*, 3740–3743. (b) Hecht, S.; Meudtner, R. M. *Angew. Chem., Int. Ed.* **2008**, *47*, 4926–4930.
- (9) (a) Farnham, W. B.; Roe, D. C.; Dixon, D. A.; Calabrese, J. C.; Harlow, R. L. *J. Am. Chem. Soc.* **1990**, *112*, 7707–7718. (b) Zhu, S. S.; Staats, H.; Brandhorst, K.; Grunenberg, J.; Gruppi, F.; Dalcanele, E.; Luetzen, A.; Rissanen, K.; Schalley, C. A. *Angew. Chem., Int. Ed.* **2008**, *47*, 788–792. (c) Hay, B. P.; Bryantsev, V. S. *Chem. Commun.* **2008**, 2417–2428. (d) Yoon, D. W.; Gross, D. E.; Lynch, V. M.; Sessler, J. L.; Hay, B. P.; Lee, C. H. *Angew. Chem., Int. Ed.* **2008**, *47*, 5038–5042. (e) Berryman, O. B.; Sather, A. C.; Hay, B. P.; Meisner, J. S.; Johnson, D. W. *J. Am. Chem. Soc.* **2008**, *130*, 10895–10897.
- (10) Katayev, E. A.; Ustynyuk, Y. A.; Sessler, J. L. *Coord. Chem. Rev.* **2006**, *250*, 3004–3037, and references therein.
- (11) See Supporting Information.
- (12) Alderighi, L.; Gans, P.; Ienco, A.; Peters, D.; Sabatini, A.; Vacca, A. *Coord. Chem. Rev.* **1999**, *184*, 311–318.
- (13) (a) Vander Griend, D. A.; Bediako, D. K.; DeVries, M. J.; DeJong, N. A.; Heeringa, L. P. *Inorg. Chem.* **2008**, *47*, 656–662. (b) Li, Y.; Vander Griend, D. A.; Flood, A. H. *Supramol. Chem.* **2009**. In press.
- (14) Hirose, K. In *Analytical Methods in Supramolecular Chemistry*; Schalley, C. A., Ed.; Wiley-VCH: Weinheim, Germany, 2007.
- (15) Scatchard, G. *Ann. N.Y. Acad. Sci.* **1949**, *51*, 660–672.

JA8077329